Experimental study on resonance frequency enhancement of strong optical injection-locked semiconductor lasers

Peng Guo (郭 芃) and Zhangyuan Chen (陈章渊)*

State Key Laboratory of Advanced Optical Communication Systems and Networks, Peking University, Beijing 100871, China

**Corresponding author: chenzhy@pku.edu.cn*

Received September 23, 2013; accepted November 5, 2013; posted online December 9, 2013

Enhancing resonance frequency of strong optical injection-locked semiconductor lasers is experimentally studied. Resonance frequency is increased from 4.1 to 53.9 GHz by the optical injection locking (OIL) technique. We experimentally demonstrate that resonance frequency is strictly equal to the frequency spacing between the cavity modes of the master and slave lasers under strong OIL condition. This result provides valuable information to improve OIL theory.

OCIS codes: 140.3520, 250.5960.

doi: 10.3788/COL201311.121403.

Optical injection locking (OIL) has been demonstrated as a useful technique to enhance the modulation performance of semiconductor lasers (SLs). Theoretical work based on standard OIL rate equations first proposed by Lang in 1982[1] has been developed well during the past three decades[2−9]. Numerous novel characteristics of OIL-SLs have been theoretically investigated, including enhanced resonance frequency, enhanced radio frequency (RF) signal gain, reduced relative intensity noise, enlarged spurious free dynamic range, and reduced chirp[10]. Recently, we experimentally demonstrated three novel applications based on OIL-SLs: long distance transmission[11], phase modulation[12], and RF conversion[13]. Based on the aforementioned theoretical and experimental research, one of the most distinguished features of OIL-SLs is determined to be frequency response enhancement. Under strong OIL condition, the resonance frequency of directly modulated (DM) OIL-SLs can reach >100 GHz[14]. Numerous high-frequency response applications of DM-OIL-SLs are demonstrated based on this novel characteristic, such as radio over fiber[15] and optoelectronic oscillator[16]. The three kinds of typical theoretical results of resonance frequency enhancement of OIL-SLs are as follows: rigorous analytical solution with complex formula expression[2,3]; approximate solution with simpler formula expression[4,5], as shown in Eq. (1); intuitive solution with the simplest formula expression[6,7], as shown in Eq. (2).

$$f_{\mathrm{R}} = \sqrt{(c\Delta\lambda'/\lambda_0^2)^2 + f_{\mathrm{fr}}^2}, \quad (1)$$

$$f_{\mathrm{R}} = c\Delta\lambda'/\lambda_0^2. \quad (2)$$

The relevant parameters are defined in Table 1. One explanation for Eq. (2) is that resonance frequency is produced by the interference between master and slave lasers[6]. Another explanation is that the cavity mode region of OIL-SLs selectively amplifies one sideband of the "externally modulated" master laser[7]. In the present study, OIL-SL is regarded as an external modulator based on our external modulator model for OIL-SLs[17]. Both explanations show that enhanced resonance frequency strictly corresponds to the frequency difference between the OIL wavelength and the cavity mode of the slave laser. Equation (2) is typically considered as the approximate expression of Eq. (1). In this letter, however, we experimentally demonstrate that the accuracy of Eq. (2) is superior to that of Eq. (1). This result provides significant value to improve OIL theory.

To verify the relationship between f_{R} and $\Delta\lambda'$ in Eq. (2), the experimental setup is shown in Fig. 1. A commercial EM4 high-power distributed feedback (DFB) laser is used as the master laser. This DFB laser is a continuous-wave (CW) InGaAsP/InP multi-quantum well laser diode. The slave laser is a single-mode 1550 nm vertical-cavity surface-emitting laser (VCSEL) designed with a buried tunnel junction structure to confine both current and light. The injection of the master laser locks the slave laser through an optical circulator (OC). A polarization controller is used to match the polarization of the master laser to the different polarization modes of the VCSEL. The output light from the VCSEL passes through the OC and through an optical splitter (OS).

Table 1. Parameters Used in Eqs. (1) and (2)

Parameter	Symbol
Resonance Frequency under Free-running Wavelength (GHz)	f_{fr}
Resonance Frequency under Injection Locking (GHz)	f_{R}
Velocity of Light in a Vacuum (m/s)	c
Slave Laser Free-running Wavelength (nm)	λ_0
Slave Laser Cavity Wavelength under Injection Locking (nm)	λ_{s}
Master Laser Wavelength (nm)	λ_{m}
Wavelength Difference between Master and Slave Lasers under Injection Locking (nm)	$\Delta\lambda' = \lvert\lambda_{\mathrm{s}} - \lambda_{\mathrm{m}}\rvert$

One output port of the OS is sent to the optical spectrum analyzer (OSA) to monitor the spectrum. The other output port is sent directly to the network analyzer.

Figure 2 shows the frequency responses under different strong OIL conditions. The wavelength of the master DFB laser is strongly dependent on the temperature controller. The wavelength increases by $\sim$ 0.1 nm with each 1 °C increase in temperature. The OIL parameters (wavelength detuning: $\Delta\lambda$ and injection ratio: R_{inj}) are optimized to obtain different resonance frequencies. To obtain the largest resonance frequency, a high injection ratio is generally required. For example, under OIL condition 1 shown in Fig. 3, the OIL parameters are optimized at –0.322 nm wavelength detuning ($\lambda_{\text{master}} = 1546.994$ nm, $\lambda_{\text{slave}} = 1547.316$ nm) and 16.9 dB injection ratio ($P_{\text{master}} = 12.4$ dBm, $P_{\text{slave}} = -4.5$ dBm). The largest resonance frequency ($f_{\text{R}} = 53.9$ GHz) is achieved under this condition. Moreover, we keep the peak of resonance frequency sharp enough during the entire experiment to distinguish the resonance frequency (f_{R}) easily from the frequency response curves in Fig. 2.

Figure 3 shows the comparison between frequency response curves and spectra under different conditions. The gray curves are plotted under the free-running (FR) condition. The VCSEL is biased at 8.0 mA to yield a –4.5-dBm output power at room temperature (293.0 K). The wavelength of VCSEL is 1547.316 nm and resonance frequency is 4.122 GHz under this condition. The red curves are plotted under OIL condition, and the serial numbers in Fig. 3 (i.e., 1, 7, and 13) correspond with those in Fig. 2. Frequency response enhancement by OIL can be evidently verified in Fig. 3(a).

f_{R} and $\Delta\lambda'$ (defined in Table 1) are extracted from Fig. 3 and plotted in red hollow points in Fig. 4. To validate the theoretical results of Eqs. (1) and (2), the blue dotted curve of Eq. (1) and the black line of Eq. (2) are plotted for comparison. To verify the relationship between f_{R} and $\Delta\lambda'$ clearly, the difference between the black line and the blue dotted line can be better distinguished by using low f_{R}, as shown in Fig. 4(b). However, the resolution of our OSA in the experiment limits the minimum measurable $\Delta\lambda'$. Nevertheless, Fig. 4(b) clearly shows that the accuracy of Eq. (2) is superior to that of Eq. (1).

In conclusion, we experimentally demonstrate that resonance frequency enhancement by OIL is strictly equal to the frequency spacing between the master and slave lasers under strong OIL condition. The experimental result verifies the accuracy of the amplifier model of OIL-SLs. On the other hand, this result provides valuable information to improve OIL theory.

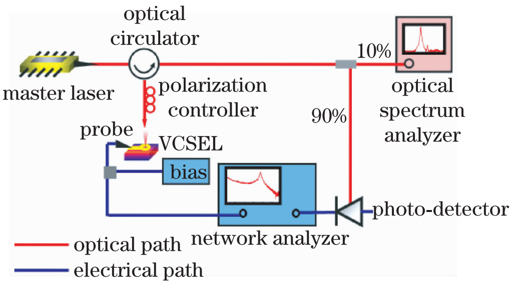

Fig. 1. (Color online) Experimental setup of the frequency response measurement and optical spectrum collection of OIL-VCSEL.

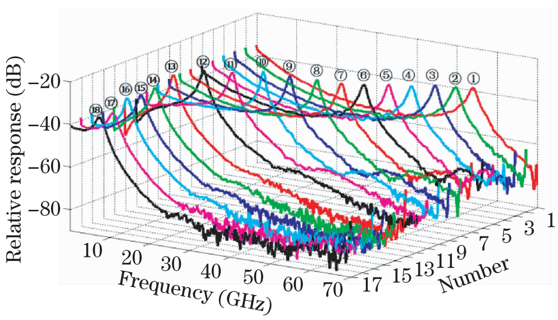

Fig. 2. (Color online) Frequency responses of OIL-VCSEL under different strong OIL conditions.

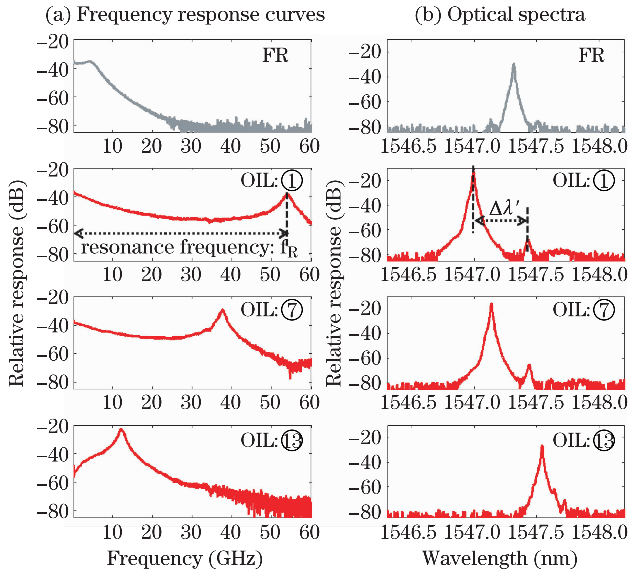

Fig. 3. Comparison between f_{R} and $\Delta\lambda'$ under different experimental conditions: FR, OIL (1, 7, and 13 in Fig. 2). (a) frequency response curves; (b) optical spectra.

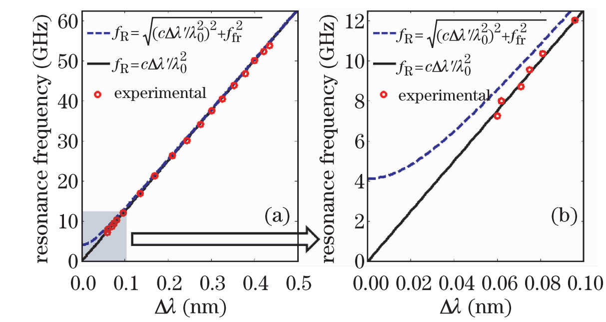

Fig. 4. (Color online) Comparison between the theoretical and the experimental results. (a) Resonance frequency enhancement by OIL; (b) close up of the shaded part of Fig. 4(a).

This work was supported by the National “973” Program of China (Nos. 2012CB315606 and 2010CB328201).

References

1. R. Lang, IEEE J. Quantum Electron. **18,** 976 (1982).
2. L. L. Li, IEEE J. Quantum Electron. **30,** 1701 (1994).
3. J. Wang, M. K. Haldar, L. Li, and F. V. C. Mendis, IEEE Photon. Technol. Lett. **8,** 34 (1996).

4. C. Henry, N. Olsson, and N. Dutta, IEEE J. Quantum Electron. **21,** 1152 (1985).
5. E. K. Lau, H. K. Sung, and M. C. Wu, IEEE J. Quantum Electron. **44,** 90 (2008).
6. A. Murakami, K. Kenta, and A. Kazuhiko, IEEE J. Quantum Electron. **39,** 1196 (2003).
7. X. Zhao and C. J. Chang-Hasnain, IEEE Photon. Technol. Lett. **20,** 395 (2008).
8. P. Guo, W. Yang, D. Parekh, A. Xu, Z. Chen, and C. J. Chang-Hasnain, Opt. Express **20,** 6980 (2012).
9. P. Guo, W. Yang, D. Parekh, C. J. Chang-Hasnain, A. Xu, and Z. Chen, Opt. Express **21,** 3125 (2013).
10. E. K. Lau, L. J. Wong, and M. C. Wu, IEEE J. Sel. Top. Quantum Electron. **15,** 618 (2009).
11. P. Guo, C. Zhang, J. Li, W. Yang, D. Parekh, C. J. Chang-Hasnain, W. Hu, A. Xu, and Z. Chen, Chin. Opt. Lett. **10,** 091407 (2012).
12. P. Guo, T. Sun, W. Yang, D. Parekh, C. Zhang, X. Xie, C. J. Chang-Hasnain, A. Xu, and Z. Chen, Opt. Express **21,** 22114 (2013).
13. P. Guo, C. Zhang, A. Xu, and Z. Chen, Opt. Express **21,** 7276 (2013).
14. E. K. Lau, X. Zhao, H. K. Sung, D. Parekh, C. J. Chang-Hasnain, and M. C. Wu, Opt. Express **16,** 6609 (2008).
15. A. Ng'oma, D. Fortusini, D. Parekh, W. Yang, M. Sauer, S. Benjamin, W. Hofmann, M. C. Amann, and C. J. Chang-Hasnain, J. Lightwave Technol. **28,** 2436 (2010).
16. H. K. Sung, X. Zhao, E. K. Lau, D. Parekh, C. J. Chang-Hasnain, and M. C. Wu, IEEE J. Sel. Top. Quantum Electron. **15,** 572 (2009).
17. P. Guo, L. Zhu, A. Xu, and Z. Chen, in *Proceedings of Opto Electronics and Communications Conference* TuPK-9 (2013).